Real-time fast ultrasonic monitoring of cracking in a concrete cylinder subject to compression

Cédric Dumoulin[1], Arnaud Deraemaeker[1]
[1]Université Libre de Bruxelles, BATir Department, 50 av F D Roosevelt, CP 194/02,
B-1050 Brussels, Belgium
email: aderaema@ulb.ac.be

ABSTRACT: The field of structural health monitoring and damage detection has been studied intensively for the last thirty years due to the aging of expensive critical components for safety, mainly in the field of aeronautics and civil engineering. Such systems rely on dynamic signatures of structures which are either generated by the ambiance, or generated by the monitoring system itself. The latter solution can provide more local information on damages since the monitoring system can generate high frequency (ultrasonic) signals. Ideal candidates for the generation of such signals are piezoelectric PZT transducers, due to their small size, low cost and large bandwidth. Embedded piezoelectric transducers (Smart Aggregates) have been recently developed for concrete applications. In this study, these transducers are used to assess the damage in a concrete cylinder subject to compression. In the past, these transducers produced in the Civil Engineering Laboratory at ULB-BATir have been successfully used both for in-situ estimation of the P-Wave velocity at early age of concrete and for crack monitoring. The previous monitoring system has the limitation of being very slow and not adequate to monitor fast behavior alteration. In this study, we develop a completely new and fast data acquisition system which enables to reach up to 150 ultrasonic measurements per second. The efficiency of the system is demonstrated on a concrete cylinder with a pair of embedded transducers which is monitored under compression until failure.

KEY WORDS: Non Destructive Testing, Concrete Damage Monitoring, Fast Sensing, Embedded Piezoelectric Transducers, Smart Aggregates, Acoustic Emission Event

1 INTRODUCTION

Several factors can affect a concrete structure and can lead it to be turned out of service or in the most dramatic cases to the complete failure. To avoid such kind of situation it is important to evaluate regularly the state of the structure. In the past, visual inspection and destructive tests were the only possibilities for assessing the state of the structure. The number of inspections was really reduced due to the cost related to these tests. Furthermore, it only allowed a macroscopic identification of damage at accessible places. The recent development of Non Destructive Tests (NDT) has given the opportunity of more automatic tests that greatly improves the repeatability and the efficiency of the tests. Nowadays, large structures are commonly monitored by several sensors as strain gauges, temperature sensors, etc. The field of structural health monitoring for civil engineering structure can be divided in two main different domains. The first is the detection of large scale effects by analyzing the firsts vibration modes excited by ambient vibration (wind, traffic…) using accelerometers or more recently fiber optic dynamic strain sensors [1]. The second domain is more focused on local damages for which higher frequencies analysis is needed. For such type of signals, ideal candidates are piezoelectric PZT transducers, due to their small size, low cost and large bandwidth.

During the last twenty years, ultrasonic techniques have started to be applied to concrete structures using first surface mounted devices [2]. More recently the concept of Smart Aggregates (SMAGs) has been developed by researchers at the University of Houston [3]. SMAGs are embedded piezoelectric transducers. This concept has among others the advantages of the flexibility in the choice of their location in the structure and a better integration in the design of the structure. Furthermore the efficiency of these transducers is greatly improved in comparison to external transducer since it avoids the use of any coupling agent. They are composed of a thin PZT patch surrounded by several coating layers.

In the Civil Engineering Laboratory at ULB-BATir, Smart Aggregates has been developed and successfully used both for in-situ estimation of the P-Wave velocity during the setting of concrete [4] and for crack monitoring ([5], [6]).

Damage dependency of ultrasonic (US) waves in concrete specimens under compression has been extensively studied. Most of them concerned the evolution of the intensity [7] and the velocity [8] of the ultrasonic waves in the transverse direction of the load. It was demonstrated that the evolution of the intensity is more sensitive than the velocity. Recently, ultrasonic waves in the direction of the load have been used both for assessing acousto-elastic properties of concrete at low level of load [9] and microcraking monitoring [10]. Performing such ultrasonic tests requires either the modifications of the loading plates or the addition of an intermediate ring in order to set up the external ultrasonic transducers.

In this study two Smart Aggregates are cast in a concrete cylinder under compression. The use of such embedded transducers has the great advantage of avoiding modifications in the loading equipment.

In a previous study, a damage indicator has been defined [5]. It has been used successfully for tests where tensile stresses were prevailing such as bending tests or pull-out tests. One of the main goals of the current study is the investigation of the use of this damage indicator for compression tests. Early results with compression tests show that this damage indicator is no longer suitable. It is mainly due to the acoustoelastic effect which increases the velocity with the stress intensity. In this study, other indicators such as amplitude, velocity and energy of the transmitted wave are studied with the aim of identifying those that do not seem be sensitive to with the acousto-elastic effect.

In the previous ultrasonic studies performed at ULB-BATir the main limitation was the weak measurement rate of the monitoring system. It only allowed one measurement every ten seconds which was not adapted for damage monitoring in the case of a very sudden and brutal events. In this study, a new fast low voltage monitoring system has been developed which allows to record up to 150 measurements every second. The system is used for a compression test with a cylinder where SMAGs have been cast. The results show that the fast ultrasonic monitoring system developed in this study is both suitable for ultrasonic monitoring and for the detection of acoustic events.

2 NEW MONITORING SYSTEM

The aim of the current study is to detect the appearance of cracks and to continuously follow the level of damage of a concrete structure using ultrasonic measurements. The appearance of cracks or microcracks in concrete can be a very fast, random and brutal phenomenon. In order to follow each step of deterioration of concrete during the test, the number of measurements must be very large. A short pulse excitation signal has the advantage of exciting broadband frequencies in a short time. It has been observed that response signals to such excitation signals are generally totally attenuated after 3ms. The new fast data acquisition system developed in this study is able to reach up to 150 ultrasonic measurements per second. The data acquisition card used in the system is the NI-PXI-6115. The monitoring system also uses a specific analog preamplifier designed by Smartmote. Both instruments are controlled with an in-house software based on LabVIEW environment. The main characteristics of the system are summarized on Table 1. It is important to note that the developed system is a low voltage system (10 Volts). However the system achieves a good signal-to-noise ratio especially through the performance of the preamplifier at the sensor side. The system is also designed to record average signal measurements with the goal of increasing the SNR.

3 EXPERIMENTAL PROGRAM AND SPECIMEN

The present experiment consists of an uni-axial compression test on a concrete cylinder (diameter 11.3 cm and height 22 cm). A pair of SMAGs has been cast inside the cylinder at a distance of 13 cm. The concrete used for this experiment is an ordinary concrete for which the components are described in Table 2. Six sixty millimeters strain gauges (SG) have been glued on the face of the cylinder. Three have been placed for longitudinal strain measurement and three have been used for the measurement of the transversal strain (see Figure 1). The SGs are located at 120° from each other. This eliminates the bending component from the strain measurement (see section 4 stress-strain results).

Table 1 - Characteristic of ultrasonic monitoring system

Number of outputs	2	Sampling Rate	4 M/s
Number of inputs	4	Sampling Rate	10 M/s
Output Signal	Pulse 5µs	Amplitude	10V
Duration of measurement	3ms	Measurement Rate	Up to 150 /s

Table 2 - Composition of concrete.

Constituent	Density [kg/m³]
Cement (CEM I 52.5 N PMES CP2)	340
Sand (Bernière 0/4)	739.45
Aggregates (Bernière 8/22)	1072.14
Water	184.22

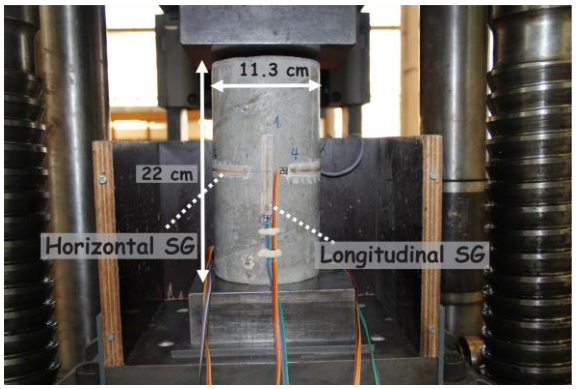

Figure 1 – Specimen. The diameter of the cylinder is 11.3 cm and the height is 22 cm. The strain gauges are disposed at 120° from each other around the cylinder.

The loading machine used for the experiment is a 1000kN hydraulic jack compression machine (see Figure 2). The machine is controlled by a digital controller (Digicon). The reaction of such machine is very slow and makes hazardous the measurement of the complete softening curve. Since the main goal of the test was to evaluate the evolution of the damage level with the load increase using ultrasonic techniques, it was decided to control the test in force. The loading rate has been fixed at 0.5 kN/s which corresponds (in the linear part) to a strain rate of 0.1 10−3/s. This is an usual recommendation for uni-axial concrete tests [11].

The force, the displacement and the strains have been recorded on a computer using a NI DAQ system, respectively the NI PXI-4461 card for the displacement and the force measurements and the NI PXIe-4330 card for the strain

gauges measurements. The SGs have been wired with a quarter-bridge configuration.

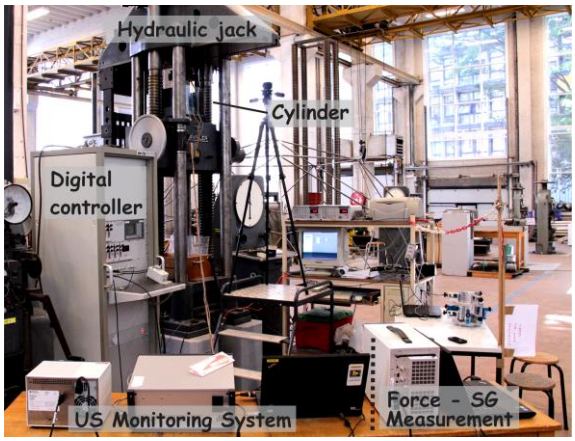

Figure 2 - Loading machine - hydraulic jack controlled by Digicon.

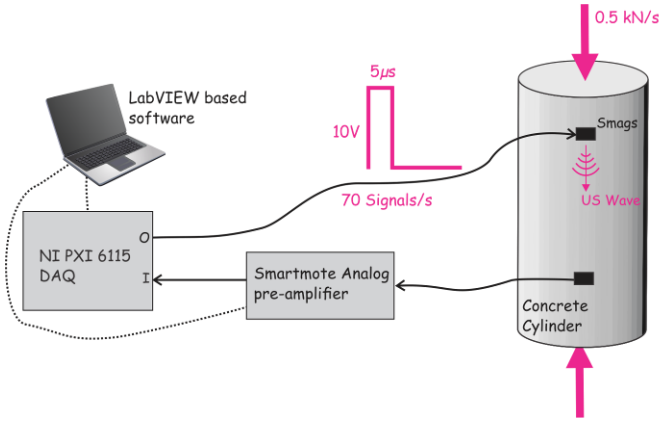

Figure 3 – Monitoring system developped for fast damage monitoring at low voltage.

The ultrasonic measurement rate has been fixed at 70 measurements every second. The excitation signal is a low voltage short pulse (5µs, 10V). The duration of each measurement is 3ms which allows a complete attenuation of the ultrasonic wave in the cylinder before the next measurement. The test is summarized on Figure 3.

4 STRESS-STRAIN RESULTS

The force-strain curves are given on Figure 4 (longitudinal strain) and Figure 5 (transversal strain). The value of each strain gauge (SG) and the mean value are shown both for the longitudinal and transverse strains measurement. One can observe the dispersion between the different SGs. It mainly results of the small decentering of the load and the non-symmetric appearance of damage due to initial weak zones [12]. In order to properly interpret the evolutions in the ultrasonic waves, it is essential to understand the failure mechanism of the cylinder. It can be observed in Figure 6 that the failure mode seems to be a mixed mode with splitting (longitudinal cracks) and shear failure.

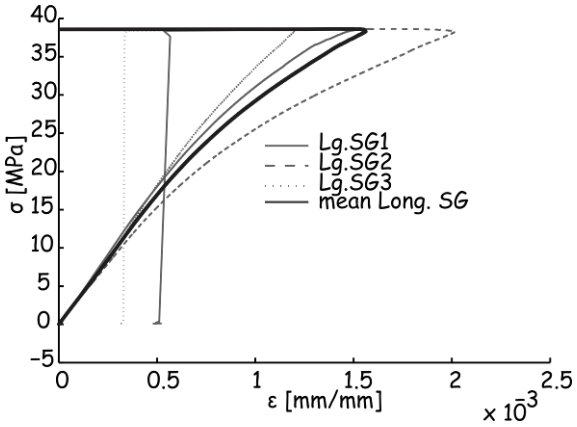

Figure 4 – Longitudinal strain measured with 3 strain gauges disposed at 120° around the cylinder

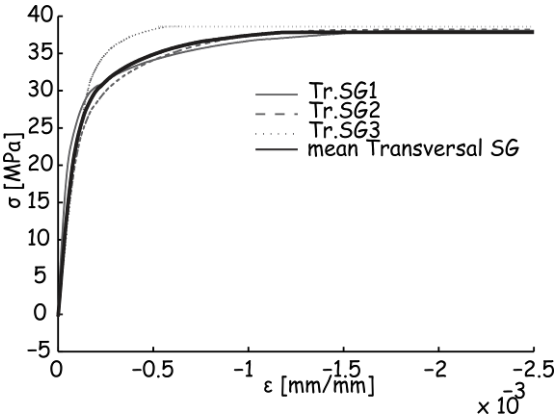

Figure 5 - Transversal strain measured with 3 strain gauges disposed at 120° around the cylinder

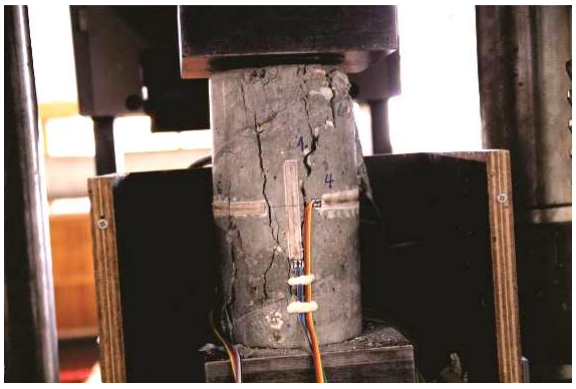

Figure 6 - Failure mechanism of the cylinder. The failure mode is a mixed mode with splitting and shear failure

5 ULTRASONIC RESULTS

This section aims to present the analysis of the ultrasonic signals. The first part is dedicated to the detection of Acoustic Events. Indeed, the important number of US measurements has allowed the observation of Acoustic Emission Events in addition to measured ultrasonic tests. Next, the early wave damage index as defined in [5] will be analyzed. In the third part the evolution of the ultrasonic pulse velocity will be

illustrated, then the evolution of the amplitude of the signal and finally the evolution of the energy contained in the signal will be discussed. For each case the results are compared with the evolution of the strains.

5.1 Acoustic Emission events detection

The high ultrasonic measurement rate has allowed the detection of acoustic emission events (AE). Such events are undesirable effects for accurately analyzing ultrasonic signals especially since the amplitude of these events is of the same order of magnitude as the transmitted ultrasonic signals (see Figure 7). These parasite signals are produced by the appearance of damage in the structure and as a consequence the number of AE events is a good indicator for damage assessment. It was therefore decided to count these parasites signals.

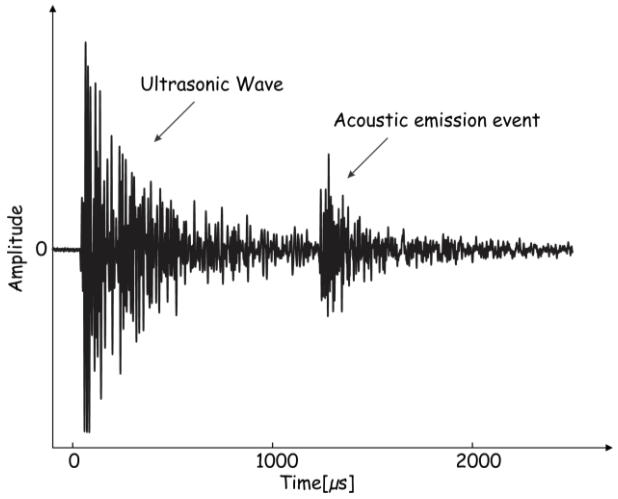

Figure 7 - Ultrasonic wave measurement parasitized by an acoustic emission event

The signals are detected by comparing the energy contained is each signal with the average of the last ten sane signals (without AE parasites) preceding the analyzed signal. The value of the RMSD (Root Main Square Deviation) between these signals (Equation 1) is used as criterion for comparison.

$$AE_j = \sqrt{\frac{\int_0^{t_f}(x_j(t)-x_m(t))^2 dt}{\int_0^{t_f} x_m^2(t) dt}} \qquad (1)$$

where $x_j(t)$ and $x_m(t)$ are respectively the signal j and the local averaged signal. t_f is the last sample of the measured signal.

This indicator approaches zero when the signals are the same. When the indicator is noticeably higher than its baseline value that is generally 0.1 to 0.2 it is considered that an acoustic event has been observed. The baseline value of the indicator results of small differences and the noise that necessarily differentiates two successive signals even when they are both sane.

The cumulative sum of the number of detected acoustic event is presented on Figure 8. It can be observed that the number of AE grows exponentially in the non-linear part of the stress-strain curve.

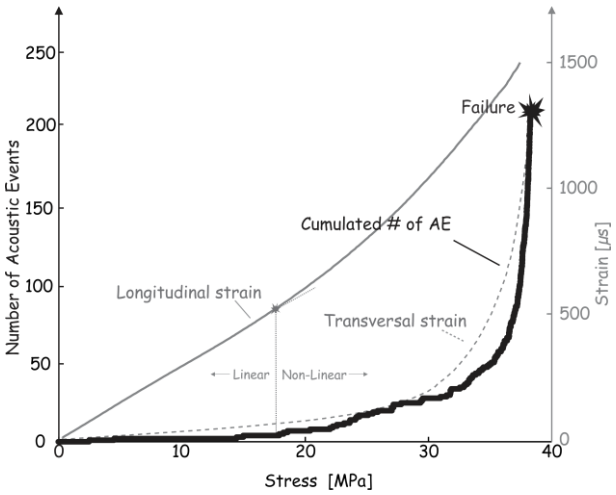

Figure 8 - Evolution of the cumulated sum of AE events with the compressive stress in comparison to the strain

5.2 Early wave Damage Index

This damage indicator is based on the simple reasoning that the first period of the recorded wave corresponds to the shortest wave path, which is affected only by the mechanical properties of the concrete between the transducers. The damage indicator is defined by the RMSD value between the healthy signal and a damaged signal computed in the time window corresponding to the first half-period of the undamaged signal (Equation 2):

$$I_j = \sqrt{\frac{\int_{t_1}^{t_2}(x_j(t)-x_0(t))^2 dt}{\int_{t_1}^{t_2} x_0^2(t) dt}} \qquad (2)$$

where $x_j(t)$ and $x_0(t)$ are respectively the signal j and the original undamaged signal. $t_1$and t_2 correspond to the limits of the first half period of the healthy signal.

The general trend of the evolution of this indicator (Figure 9) can give information on the level of damage. Indeed, it increases continuously and it stabilizes after a certain load which approximately corresponds to the limit of the linear part of the force-strain curve. Nevertheless this indicator is expected to tend to one as the damage. Unfortunately, it is not the case here due to the acousto-elastic effect.

The acousto-elastic effect is the relation between the stress intensity and the wave velocity in the material. For an uni-axial test the relation is given by Equation 3 [13]

$$V_{ij} = V_{ij,0}\left(1 - A_{ij}\,\sigma_{zz}\right) \qquad (3)$$

where V_{ij} is the velocity of the wave in direction i and polarization in direction j and A_{ij} is the corresponding

acousto-elastic constants. σ is the stress ($\sigma > 0$ corresponds to a tensile stress) and z is the direction of the load. For concrete the value of the acousto-elastic constants varies from $0.1\ 10^{-3}$ to $2\ 10^{-3}[MPa^{-1}]$ depending of the concrete formulation [14].

The damage indicator in equation 2 was built with tests in which tensile stresses were predominant. In this case the acousto-elastic effect affected the velocity in the same way as the appearance of damage (reduction of the velocity), on the contrary to a compression test. This is confirmed by analyzing the evolution of the wave velocities (see section 5.3). Furthermore the magnitude of this effect was reduced due to the weak strength of concrete to tensile stresses. The transmitted wave was therefore more affected by the appearance of damage than the acousto-elastic effect. For the compression test the level of stress is much higher and the acousto-elastic effect has a higher impact. In summary, the high level of stress implies an increase of the velocity which makes the damage indicator not suitable and demonstrates the need of new features for damage assessment.

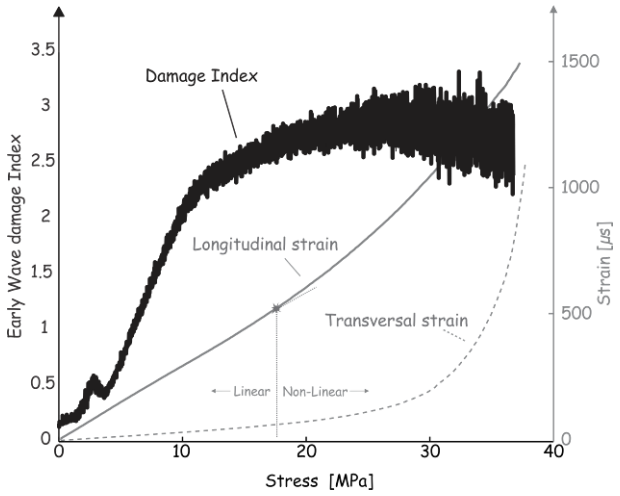

Figure 9 - Evolution of the early wave damage index with the compressive stress in comparison to the strain

5.3 Evolution of relative pulse velocity

Figure 10 shows the evolution of the relative pulse velocity during the test. The relative velocity is defined by Equation 4.

$$\nu = \frac{V - V_0}{V_0} = \frac{\delta V}{V_0} \tag{4}$$

where V is the velocity of the propagated wave, V_0 is the average velocity of the baseline signals (before any load) and δV is the deviation. The velocity is measured with TOF (Time of Flight) of the propagated wave.

During the compression test the relative velocity first increases due to the closure of the voids in the concrete. After that, the damage induces a decrease of the average stiffness and as a consequence the relative pulse velocity. It is shown that the relative velocity is stabilized after the first peak and decreases again near the failure. This behavior defines three different phases which can be compared to the phases observed by Shokouhi et al. [15].

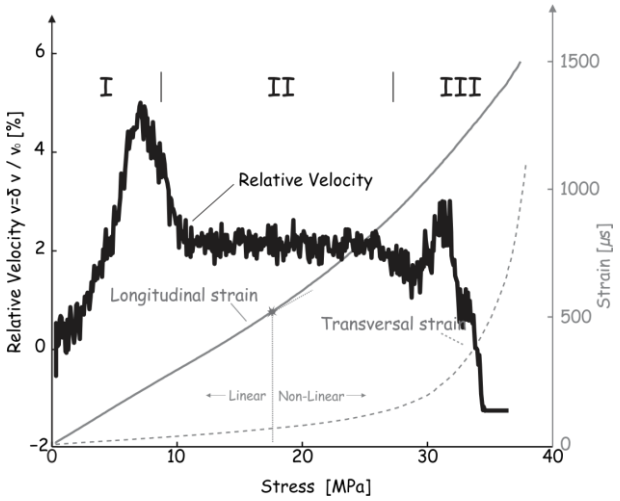

Figure 10 - Evolution of the relative velocity with the compressive stress in comparison to the strain

- Phase I: The acousto-elastic effect results in an increase in the measured velocities. The stress causes the closure of initial microcracks which leads to an increase in the stiffness and therefore the wave velocities. Appearance of damage (here in the form of new microcracks) results in a decrease of the wave velocities. Although the stress-strain curve seems to be linear it has been shown that microcracks appear when the external load is applied [12]. After a certain load the latter phenomenon gets dominant and a peak of velocity appears.

- Phase II: The relative velocity decreases due to appearance of micro-cracks. Above a certain load the velocity seems to be stabilized during a broad range of load. It can be explained by the appearance of macrocracks parallel to the load direction. Such cracks have therefore almost no impact in the wave velocity since the wave path does not change. This reasoning can be confirmed by observing the failure mechanism of the cylinder (Figure 6).

- Phase III: At high level of load all the cylinder is subjected to severe damage. It results in a fast decrease of the stiffness and therefore a fast decrease of the wave velocities until the complete failure of the cylinder.

Since the evolution of the velocity does not evolve continuously it cannot be used as such as an indicator of the evolution of the damage. As an alternative, the evolution of the amplitude will be studied in the next section.

5.4 Evolution of the amplitude

In this section the evolution of the wave velocity is compared to the evolution of the amplitude. Three different amplitudes are studied. The first is the maximum amplitude (A_m) of the

transmitted signal (Figure 11) and the two others are the amplitude of the first and the second peaks (respectively A_{m1} and A_{m2}) of the received signal (Figure 12). The results are given in terms of relative amplitude A/A_0 where A is the amplitude of the current signal and A_0 is the average amplitude of the baseline signals.

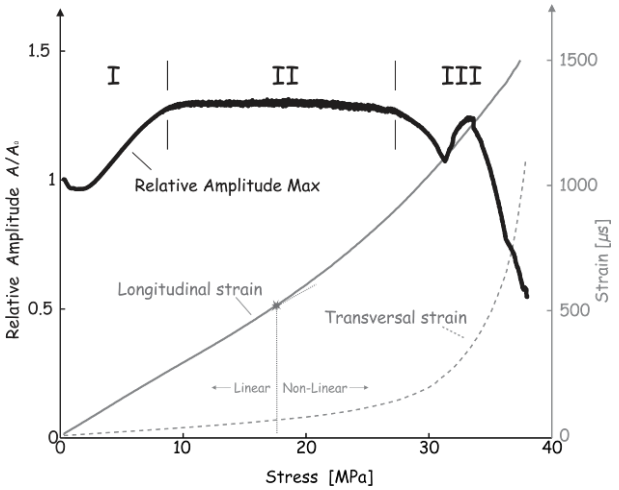

Figure 11 - Evolution of the relative amplitude of the maximum peak of the received signals with the compressive stress in comparison to the strain.

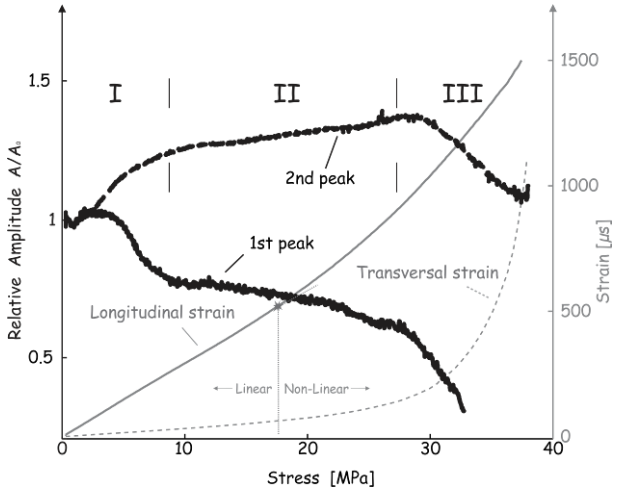

Figure 12 - Evolution of the relative amplitude of the 1st and 2nd peaks of the received signal with the compressive stress in comparison to the strain.

The phases defined in section 5.3 have also been used to analyze the evolution of the amplitudes. In phase I, until 5MPa the amplitude of A_{m1} is practically steady while A_m and A_{m2} increase. This tends to show that A_{m1} is not affected by the acousto-elastic effect and may represent only the level of damage. Consequently, A_{m1} is the only relevant damage indicator in terms of amplitude. After 5MPa, A_{m1} decreases due to the appearance of microcracks in the specimen, which is earlier than the evolution of the number of acoustic emission events in Figure 8.

In the second phase one can observe a certain dwelling step. This is due to the appearance of longitudinal macrocracks which do not strongly affect the wave path.

Finally the value of the amplitude decreases quickly in the third phase due to the generalized failure of the cylinder.

It is important to note that the amplitude of the first peak is very low after a certain load and cannot be accurately distinguished from the level of noise. Nevertheless the first peak amplitude is the most appropriate indicator since it continuously decreases with stress induced damage.

5.5 Evolution of Energy

In order to evaluate the evolution in the transmitted signal one can also compute the evolution of the total energy contained in each recorded signal. The energy of the signal is given by Equation 5:

$$E_j = \int_0^{t_f} x_j^2(t)dt \tag{5}$$

where $x_j(t)$ is the recorded signal j.

The evolution of the transmitted energy is shown on Figure 13. The results are presented in terms of relative energy E/E_0 where E is the total energy of the current signal and E_0 is the average energy of the baseline signals.

The curve is also cut in three different phases but the general trends of the three phases are less marked than previously.

This indicator is particularly difficult to interpret as it is affected by all alterations in the internal structure of the cylinder. Accordingly this indicator has no clear tendency and cannot be used to assess the level of damage.

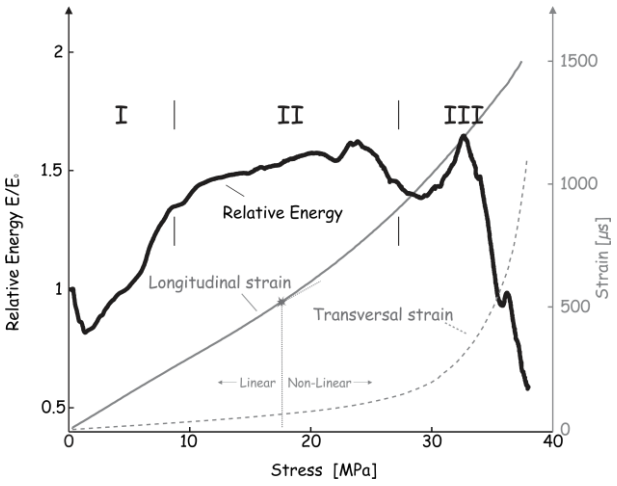

Figure 13 - Evolution of the total energy of the received signal with the compressive stress in comparison to the strain.

6 CONCLUSIONS

In this study a compression test has been performed on a cylinder in which two smart aggregates have been cast in order to evaluate damage using ultrasonic waves. It has been shown that the acousto-elastic effect has a strong impact on

the wave transmission in concrete when a high level of compressive stresses is applied.

It implies that damage index based on the evolution of the velocity of the propagated wave cannot be used since the effect of damage on the wave velocity cannot be distinguished from the acousto-elastic effect.

As an alternative, the amplitude of the signal can be used. The first peak amplitude indicator is interesting since it both continuously evolves and follows well the three different phases which describe the failure mechanisms that are the microcracks initiation, the appearance of longitudinal macrocracks and the complete failure.

It could be concluded from the results of this test that the amplitude of the first peak is more sensitive than counting the number of acoustic emission events since it evolves for lower levels of load. This interesting finding will be investigated in more details in the future.

ACKNOWLEDGMENTS

Cédric Dumoulin is a Research Fellow of the Fonds de la Recherche Scientifique - FNRS and Arnaud Deraemaeker is a Research Associate of the Fonds de la Recherche Scientifique – FNRS. This research was supported by the “Fonds David et Alice Van Buuren”.

REFERENCES

[1] A. Deraemaeker and K. Worden, *New trends in vibration based structural health monitoring*. Springer, 2010.

[2] J. Bungey, S. . Millard, and M. Grantham, *Testing of concrete in structures*, 4th ed. Taylor & Francis e-Library, 2006, 2006, p. 352.

[3] H. Gu, G. Song, H. Dhonde, Y. L. Mo, and S. Yan, “Concrete early-age strength monitoring using embedded piezoelectric transducers,” *Smart Mater. Struct.*, vol. 15, no. 6, pp. 1837–1845, 2006.

[4] C. Dumoulin, G. Karaiskos, J. Carette, S. Staquet, and A. Deraemaeker, “Monitoring of the ultrasonic P-wave velocity in early-age concrete with embedded piezoelectric transducers,” *Smart Mater. Struct.*, vol. 21, no. 4, p. 047001, 2012.

[5] C. Dumoulin, G. Karaiskos, and A. Deraemaeker, “Monitoring of crack propagation in reinforced concrete beams using embedded piezoelectric transducers,” in *VIII International Conference on Fracture Mechanics of Concrete and Concrete Structures*, 2013, pp. 1717–1725.

[6] G. Karaiskos, S. Flawinne, J.-Y. Sener, and A. Deraemaeker, “Design and validation of embedded piezoelectric transducers for damage detection applications in concrete structures,” in *10th International Conference on Damage Assessment of Structures*, 2013, no. Figure 1, pp. 1–7.

[7] W. Suaris and V. Fernando, “Detection of crack growth in concrete from ultrasonic intensity measurements,” *Mater. Struct.*, no. 20, pp. 214–220, 1987.

[8] S. Popovics and J. S. Popovics, “Effect of stresses on the ultrasonic pulse velocity in concrete,” in *2nd International RILEM Symposium on Advances in Concrete through Science and Engineering*, 1989, no. February, pp. 15–23.

[9] I. Lillamand, J.-F. Chaix, M.-A. Ploix, and V. Garnier, “Acoustoelastic effect in concrete material under uni-axial compressive loading,” *NDT E Int.*, vol. 43, no. 8, pp. 655–660, Nov. 2010.

[10] P. Shokouhi, “Monitoring of Progressive Microcracking in Concrete Using Diffuse Ultrasound,” in *6th European Workshop on Structural Health Monitoring*, 2012, pp. 1–8.

[11] S. P. Shah, J. G. M. van Mier, N. Banthia, A. Bascoul, Y. Berthaud, Z. Bittnar, O. Buyukozturk, A. Carpinteri, M. Elices, G. Ferrara, R. Gettu, K. Gylltoft, M. Hassanzadeh, N. Hawkins, H. Horii, B. L. Karihaloo, G. König, M. Kotsovos, J. Labuz, G. Markeset, H. W. Reinhardt, H. Schorn, H. Stang, K.-C. Thienel, and J.-P. Ulfkjær, “Test method for measurement of the strain-softening behaviour of concrete under uniaxial compression Recommendations 1 . INTRODUCTION AND SCOPE RILEM TECHNICAL COMMITTEES RILEM TC 148-SSC : STRAIN SOFTENING OF CONCRETE - TEST METHODS FOR,” *Mater. Struct. Constr.*, vol. 33, no. July 2000, pp. 347–351, 2000.

[12] J. G. M. Van Mier, *Fracture Processes of Concrete - Assessment of Material Parameters for Fracture Models*. CRC Press, 1996, p. 464.

[13] D. P. Schurr, J.-Y. Kim, K. G. Sabra, and L. J. Jacobs, “Damage detection in concrete using coda wave interferometry,” *NDT E Int.*, vol. 44, no. 8, pp. 728–735, Dec. 2011.

[14] T. Planès and E. Larose, “A review of ultrasonic Coda Wave Interferometry in concrete,” *Cem. Concr. Res.*, vol. 53, pp. 248–255, Nov. 2013.

[15] P. Shokouhi, A. Zoëga, H. Wiggenhauser, and G. Fischer, “Surface Wave Velocity-Stress Relationship in Uniaxially Loaded Concrete,” *ACI Mater. J.*, no. February, pp. 141–148, 2012.